SPIN-ISOSPIN EXCITATIONS AND NUCLEAR SHAPES

P. SARRIGUREN, E. MOYA DE GUERRA, R. ALVAREZ-RODRIGUEZ, A. ESCUDEROS

Instituto de Estructura de la Materia, C.S.I.C.
Serrano 123, 28006 Madrid, Spain

We study spin-isospin nuclear excitations using a deformed HF+BCS+QRPA formalism with residual interactions in both particle-hole and particle-particle channels. We address different problems of interest in nuclear structure and nuclear astrophysics, such as the $\beta-$decay properties of proton-rich medium-mass nuclei, the Gamow-Teller strength distributions in stable nuclei in the iron mass region, and the energy distributions of the spin magnetic dipole $M1$ strength stressing the similarities and differences with their Gamow-Teller counterparts.

1. Introduction

One of the most exciting challenges in Nuclear Physics at present is the understanding of nuclear systems under extreme conditions. The new experimental facilities using beams of exotic nuclei and the corresponding theoretical efforts to describe them are of great interest, especially in nuclear structure physics and nuclear astrophysics. Nuclear β-decay and electron capture processes are essential ingredients in calculations of supernova formation. As an example, the decay properties of proton rich nuclei are fundamental to understand the rp process, which is responsible for the nucleosynthesis of heavy proton-rich nuclei. As another example, the Gamow-Teller (GT) properties of nuclei in the iron-mass region are of special importance because they are the main constituents of the stellar core in presupernovae formations.

Our theoretical framework[1,2,3,4] is as follows: We construct first the quasiparticle basis self-consistently from a deformed HF calculation with density-dependent Skyrme forces and pairing correlations. Then we solve the QRPA equations with a separable residual interaction derived from the same Skyrme force. In this work, we first apply our formalism to the study of a series of proton rich isotope chains approaching $N = Z$ in the mass region $A = 70$. We study even-even and odd-A isotopes and compare our results to available data for Gamow-Teller strength distributions and half-lives. We also discuss the sensitivity of our calculations to deformation, pairing, and residual interactions. A second application of our formalism is made to nuclei in the iron mass region. We compare our Gamow-Teller strength distributions with data extracted from (n,p) charge exchange reactions, as well as with other theoretical results. In addition to the GT transitions we also study the spin magnetic dipole excitations on stable nuclei and compare them to available experimental information obtained from inelastic proton scattering.

2. Selfconsistent Skyrme HF+BCS+QRPA formalism in deformed nuclei

It is well known that the density-dependent HF approximation gives a very good description of ground-state properties for both spherical and deformed nuclei [5,6] and it is at present the most reliable mean field description. We consider in this paper two different Skyrme forces, Sk3 [7] and SG2 [8]. Both forces were designed to fit ground state properties of spherical nuclei and nuclear matter properties but, in addition, the force SG2 gives a good description of GT excitations in spherical nuclei.

The single-particle HF solutions for axially symmetric deformed nuclei are characterized by the eigenvalue Ω_j of the third component of the total angular momentum and parity π_j. They are expanded into the eigenfunctions of an axially deformed harmonic-oscillator potential

$$\Phi_j^t(\mathbf{R},\sigma,q)=\chi_t(q)\sum_\alpha C_\alpha^{j,t}\varphi_\alpha(\mathbf{R},\sigma)\ . \tag{1}$$

with α denoting the set of quantum numbers $\alpha\equiv\{N,n_r,n_z,\Lambda,s\}$. Truncation effects are minimized by a proper choice of the oscillator parameters of the basis. The basis space consists of eleven harmonic oscillator major shells N.

We include pairing between like nucleons in the BCS approximation with fixed gap parameters for protons Δ_π, and neutrons Δ_ν. The BCS equations are solved iteratively at the end of each HF iteration to determine the Fermi levels and occupation probabilities. The fixed gap parameters are determined phenomenologically from the odd-even mass differences through a symmetric five term formula involving the experimental binding energies.

For odd-A nuclei, the fields corresponding to the different interactions were obtained by doing one iteration from the corresponding selfconsistent field of the closest even-even nucleus, selecting the orbital occupied by the odd nucleon according to the experimental spin and parity. For those cases where this experimental assignment is not well established we choose the orbital closer to the Fermi level.

To describe Gamow-Teller transitions we add to the mean field a spin-isospin residual interaction, which is expected to be the most relevant force for that purpose. This interaction contains two parts, particle-hole (ph) and particle-particle (pp). The ph part is responsible for the position and structure of the GT resonance [9,1,2] and is derived selfconsistently from the same energy density functional (and Skyrme interaction) as the HF equation, in terms of the second derivatives of the energy density functional with respect to the one-body densities. The ph residual interaction is written in a separable form by averaging the Landau-Migdal resulting force over the nuclear volume, as explained in Ref. [1,10].

$$V_{GT}^{ph}=2\chi_{GT}^{ph}\sum_{K=0,\pm1}(-1)^K\beta_K^+\beta_{-K}^-\ ,\qquad \beta_K^+=\sum_{\pi\nu}\langle\nu|\sigma_K|\pi\rangle\, a_\nu^+a_\pi\ . \tag{2}$$

The coupling strength χ_{GT}^{ph} is determined by the Skyrme parameters, the nuclear radius, and the Fermi momentum [1]

$$\chi_{GT}^{ph}=-\frac{3}{8\pi R^3}\left\{t_0+\frac{1}{2}k_F^2\left(t_1-t_2\right)+\frac{1}{6}t_3\rho^\alpha\right\}=\frac{3G_0'}{2\pi R^3N_0}\ , \tag{3}$$

The particle-particle part is a neutron-proton pairing force in the $J^\pi=1^+$ coupling channel. We introduce this interaction in the usual way [11,9,2], that is, in terms of a separable force with a coupling constant κ_{GT}^{pp}, which is fitted to the phenomenology.

$$V_{GT}^{pp}=-2\kappa_{GT}^{pp}\sum_K(-1)^KP_K^+P_{-K}\ ,\qquad P_K^+=\sum_{\pi\nu}\left\langle\pi\left|(\sigma_K)^+\right|\nu\right\rangle a_\nu^+a_{\bar\pi}^+\ . \tag{4}$$

The proton-neutron QRPA phonon operator for GT excitations in even-even nuclei is written as

$$\Gamma_{\omega_K}^+=\sum_{\pi\nu}\left[X_{\pi\nu}^{\omega_K}\alpha_\nu^+\alpha_{\bar\pi}^++Y_{\pi\nu}^{\omega_K}\alpha_{\bar\nu}\alpha_\pi\right]\ , \tag{5}$$

where ω_K are the excitation energies, and $X_{\pi\nu}^{\omega_K},Y_{\pi\nu}^{\omega_K}$ the forward and backward amplitudes, respectively. They are obtained by solving the QRPA equations. For even-even nuclei the GT transition amplitudes in the intrinsic frame connecting the QRPA ground state $|0\rangle$ $[\Gamma_{\omega_K}|0\rangle=0]$ to one phonon states $|\omega_K\rangle$ $\left[\Gamma_{\omega_K}^+|0\rangle=|\omega_K\rangle\right]$, are given by

$$\left\langle\omega_K|\beta_K^\pm|0\right\rangle=\mp M_\pm^{\omega_K}\ . \tag{6}$$

with

$$M_{-}^{\omega_K} = \sum_{\pi\nu} \left(q_{\pi\nu} X_{\pi\nu}^{\omega_K} + \tilde{q}_{\pi\nu} Y_{\pi\nu}^{\omega_K} \right) , \quad M_{+}^{\omega_K} = \sum_{\pi\nu} \left(\tilde{q}_{\pi\nu} X_{\pi\nu}^{\omega_K} + q_{\pi\nu} Y_{\pi\nu}^{\omega_K} \right) , \tag{7}$$

$$\tilde{q}_{\pi\nu} = u_\nu v_\pi \Sigma_K^{\nu\pi} , \quad q_{\pi\nu} = v_\nu u_\pi \Sigma_K^{\nu\pi} , \tag{8}$$

v's are occupation amplitudes ($u^2 = 1 - v^2$) and $\Sigma_K^{\nu\pi}$ spin matrix elements connecting neutron and proton states with spin operators

$$\Sigma_K^{\nu\pi} = \langle \nu \left| \sigma_K \right| \pi \rangle . \tag{9}$$

The partial half-life ($t_{1/2}$) for a given transition connecting the ground state of a nucleus with an excited state in the daughter nucleus is given (neglecting the Fermi strength) by

$$f\left(Z,\omega\right) t_{1/2} = \frac{D}{\kappa^2 \left| \left\langle 1_\omega^+ \left\| \beta^+ \right\| 0^+ \right\rangle \right|^2} , \tag{10}$$

where $f\left(Z,\omega\right)$ is the Fermi integral. We use $D = 6200$ s and include effective factors

$$\kappa^2 = \left[\left(g_A / g_V \right)_{\rm eff} \right]^2 = \left[0.77 \left(g_A / g_V \right)_{\rm free} \right]^2 . \tag{11}$$

The total half-life $T_{1/2}$ for allowed β decay from the ground state of the parent nucleus is given by summing over all the final states involved in the process with excitation energy below the $Q-$value,

$$T_{1/2}^{-1} = \frac{\kappa^2}{6200} \sum_\omega f\left(Z,\omega\right) \left| \left\langle 1_\omega^+ \left\| \beta^+ \right\| 0^+ \right\rangle \right|^2 . \tag{12}$$

The QRPA treatment described above is formulated for the excitations of the ground state of an even-even nucleus. When the parent nucleus has an odd nucleon, the ground state can be expressed as a 1qp state in which the odd nucleon occupies the single-particle orbit of lowest energy. Then two types of transitions are possible,

i) Phonon excitations (3qp) in which the odd nucleon acts only as a spectator. In the intrinsic frame, the transition amplitudes are basically the same as in the even-even case but with the blocked spectator excluded from the calculation,

$$\left\langle f \left| \beta_K^\pm \right| i \right\rangle_{3qp} = \left\langle \omega_K, 1qp \left| \beta_K^\pm \right| 0, 1qp \right\rangle = \mp M_\pm^{\omega_K} . \tag{13}$$

ii) The other type of transitions (1qp) are those involving the odd nucleon. We introduce as usual [12,13,9] phonon correlations to the quasiparticle transitions in first order perturbation. The transition amplitudes for the correlated states can be found for example in Ref. [9].

Once the intrinsic amplitudes $\left\langle f \left| \beta_K^\pm \right| i \right\rangle$ are calculated, the Gamow-Teller strength $B(GT)$ in the laboratory system for a transition $I_i \to I_f$ can be obtained as

$$B\left(GT^\pm\right) = \sum_{M_i, M_f, \mu} \left| \left\langle I_f M_f \left| \beta_\mu^\pm \right| I_i M_i \right\rangle \right|^2 \tag{14}$$

in units of $g_A^2/4\pi$. The initial and final states in the laboratory frame are expressed in terms of the intrinsic states $\left| \phi_K \right\rangle$ using the Bohr-Mottelson factorization [14]. In the case of even-even parent nuclei, $I_i = K_i = 0$, $I_f = 1$, and $K_f = 0, 1$, we obtain

$$B\left(GT^\pm\right) = \frac{g_A^2}{4\pi} \left\{ \delta_{K_f,0} \left\langle \phi_{K_f} \left| \beta_0^\pm \right| \phi_0 \right\rangle^2 + 2\delta_{K_f,1} \left\langle \phi_{K_f} \left| \beta_1^\pm \right| \phi_0 \right\rangle^2 \right\} . \tag{15}$$

Spin $M1$ excitations are generated by the spin part of the $M1$ operator,

$$\mathbf{M1}_\sigma = \sqrt{\frac{3}{4\pi}} \mu_N \left[g_p^s \mathbf{S_p} + g_n^s \mathbf{S_n} \right] \tag{16}$$

with $g_t^s = 0.7 g_{t,\rm free}^s$, $g_{p,\rm free}^s = 5.5855$, $g_{n,\rm free}^s = -3.8263$.

We use a similar Skyrme HF+BCS+QRPA procedure to describe the spin $M1$ excitations with $I^\pi K = 1^+1$. The relevant interaction to describe spin-flip excitations is the spin-spin residual interaction:

$$H_{SS} = K_S \left[(1+q)\ \boldsymbol{\sigma_1} \cdot \boldsymbol{\sigma_2} + (1-q)\ \boldsymbol{\sigma_1} \cdot \boldsymbol{\sigma_2}\ \boldsymbol{\tau_1} \cdot \boldsymbol{\tau_2} \right] , \tag{17}$$

where K_S and q are related to the Landau parameters, and therefore with the Skyrme parameters,

$$K_S = 8 \frac{3}{4\pi R^3} N_0^{-1} \left(G_0 + G_0' \right) \quad ; q = \frac{G_0 - G_0'}{G_0 + G_0'} . \tag{18}$$

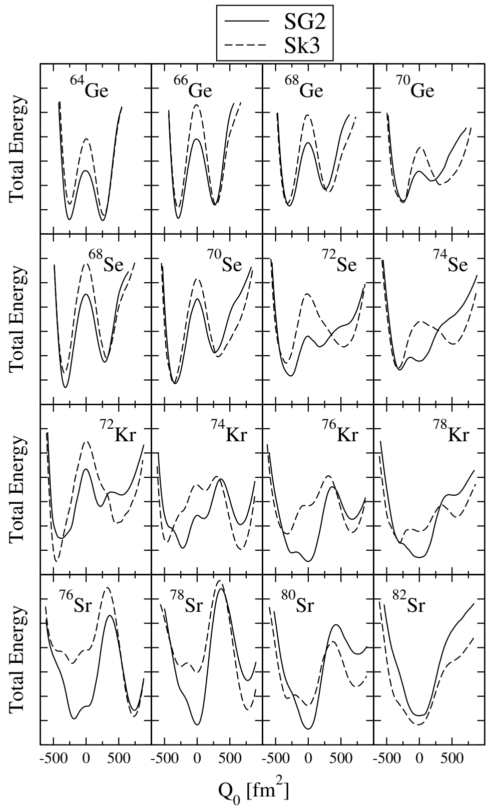

Figure 1. Total energy [MeV] of the Ge, Se, Kr, and Sr isotopes as a function of the mass quadrupole moment Q_0 [fm^2]. The results correspond to a constrained HF+BCS calculation with the Skyrme interaction SG2 (solid line) and Sk3 (dashed line). The distance between two ticks in the vertical axes is always 1 MeV but the origin is different for each curve.

3. Gamow-Teller strength distributions

The HF theory gives a single solution which is the Slater determinant of lowest energy. To allow for shape coexistence one has to extend the theory to a constrained HF theory [15]. Minimization of the HF energy under the constraint of holding the nuclear deformation fixed is carried out over a range of deformations. When more than one local minimum occurs for the total energy as a function of deformation, shape coexistence results. In Fig. 1 we show the HF energy as a function of the mass quadrupole moment for the two interactions SG2 and Sk3 in Ge, Se, Kr, and Sr isotopes. For an easier comparison in Fig. 1, the origin is different in the vertical axis for the different forces but the

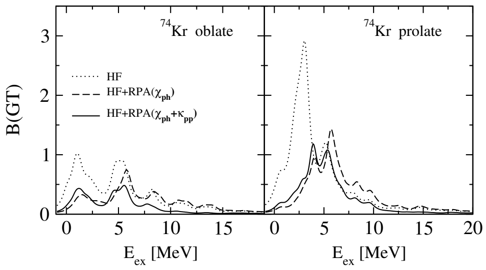

Figure 2. Gamow-Teller strength distributions in ^{74}Kr in the uncorrelated 2qp approximation (HF) and in QRPA with only ph and $ph + pp$ residual interactions.

distance between ticks corresponds always to 1 MeV. As it can be seen, we find two minima close in energy in many cases, indicating shape coexistence.

In this Section we discuss the results obtained for the GT strength distributions of the proton rich isotopes in the $A \simeq 70$ mass region, as well as of some stable nuclei in the iron mass region. The results correspond to QRPA calculations and they have been performed for the nuclear shapes that minimize the HF energy.

Figure 2 illustrates in more detail the effect of the residual interactions on the uncorrelated 2-quasiparticle calculation. If we compare first the calculation with only the ph residual interaction (dashed line) to the uncorrelated one (dotted line), we can see that the repulsive ph force shifts the strength to higher excitation energies with the corresponding displacement of the position of the GT resonance, and reduces of the total GT strength. If we now introduce a pp residual interaction (solid lines), we can see that its effect, being an attractive force, is to shift the strength to lower excitation energies, reducing the total GT strength as well. The GT strength is also pushed a bit by the pp interaction to lower energies in the low energy excitation region. This effect, although small, is relevant for the calculation of the β^+/EC half-lives, which are only sensitive to the distribution of the strength contained in the energy region below the Q_{EC} window.

In Figure 3 we can see the result of the calculation for the half-lives in ^{74}Kr as a function of the coupling strength κ_{GT}^{pp}. In the case of ^{74}Kr, we get an optimum value of $\kappa_{GT}^{pp} = 0.06$ MeV and $\kappa_{GT}^{pp} = 0.07$ MeV for the oblate and prolate shapes, respectively. We have done calculations for other cases and found that, in general, values around $\kappa_{GT}^{pp} = 0.07$ MeV improve the agreement with experiment in most cases. Since this is a valid value far from collapse, we have chosen $\kappa_{GT}^{pp} = 0.07$ MeV as the value of the coupling constant of the pp residual interaction.

The main effect of taking into account pairing correlations would be to increase the diffuseness of the Fermi surface. Since the occupation probabilities are now different from 0 or 1, the already existing peaks at $\Delta = 0$ will decrease when $\Delta > 0$, while new strength will appear at higher energies and will increase with increasing gap parameters. As a consequence, the main effect of increasing the Fermi diffuseness is to smooth out the profile of the GT strength distribution, increasing the strength at high energies and decreasing the strength at low energies.

The role of deformation on the GT strength distributions can be summarized, in general, in two types of effects. First, deformation breaks down the degeneracy of the spherical shells and this implies that the GT strength distributions corresponding to deformed nuclear shapes are much more fragmented than the corresponding spherical ones. Second, the energy levels of deformed orbitals coming from different spherical shells cross each other in a way that depends on the magnitude of the quadrupole deformation as well as on the oblate or prolate character. This level crossing may lead in some instances to sizable differences between the GT strength distributions corresponding to different shapes of the same parent nucleus. This fact can be exploited to gain information on the nuclear shape of a nucleus by just looking at the structure of its β-decay.

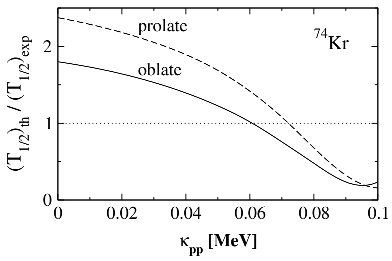

Figure 3. Ratios of calculated to experimental half-lives in ^{74}Kr as a function of the coupling strength κ_{GT}^{pp} of the particle-particle force.

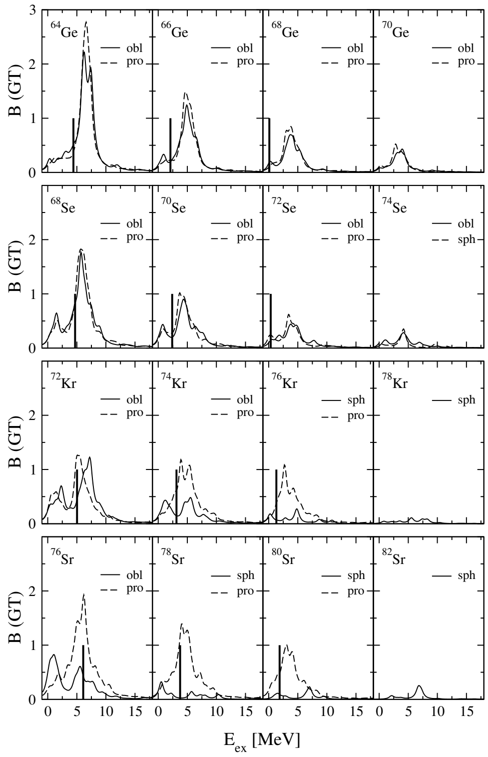

Figure 4. Gamow-Teller strength distributions $[g_A^2/4\pi]$ as a function of the excitation energy of the daughter nucleus [MeV]. The results are for the force SG2 in QRPA and for the various shapes of the isotopes ^{64,66,68,70}Ge, ^{68,70,72,74}Se, ^{72,74,76,78}Kr, and ^{76,78,80,82}Sr. Vertical lines indicate experimental Q_{EC} values.

Figure 4 summarizes these results. It corresponds to the $B(GT^+)$ strength distributions in the isotope chains of Ge, Se, Kr, and Sr, obtained from our HF+BCS+QRPA with SG2. In the case of Ge and Se isotopes, we can see that there are no signatures of the actual character, oblate or prolate, of the deformation of the parent nucleus. Both equilibrium shapes produce similar GT profiles independently of whether it is oblate or prolate. On the other hand, the figures corresponding to Kr and Sr isotopes, show differences in the GT profiles of the various shapes for each isotope that can be easily identified even within the Q_{EC} window, plotted as a vertical solid line. A case by case analysis allows one to conclude that the most favorable candidates to look for deformation effects based on β-decay measurements are ^{74}Kr and ^{76,78}Sr.

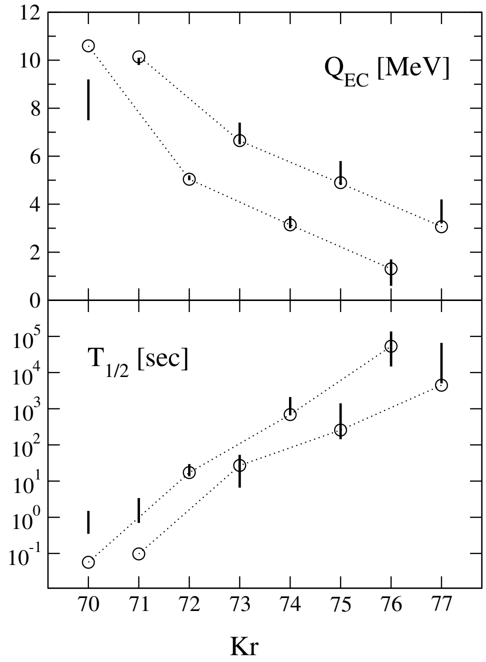

Figure 5. Experimental Q_{EC} values (top) and half-lives (bottom) for the Kr isotopes are given by circles. The solid vertical lines correspond to our theoretical QRPA calculations. The lengths of the vertical lines indicate the different results we obtain from using the forces SG2 and Sk3 and the possible shapes in each isotope.

4. Comparison with experiment

We compare to experiment our calculated Q_{EC} and total β^+/EC half-lives $T_{1/2}$, as well as the $B(GT^+)$ strength distribution in some particular cases.

Experimental Q_{EC} and $T_{1/2}$ values are plotted as circles in Fig. 5 for the Kr and Sr isotopes considered in this work. The data have been taken from Ref. [16]. These values are compared to our theoretical results represented by the vertical lines. The extreme values of these vertical lines correspond to the results obtained from the various shapes using the forces SG2 and Sk3. This has been done in order to have a better idea of the theoretical spread of the results. The agreement is in general good for both Q_{EC} and half-lives. Q_{EC} values are well reproduced with the exception of ^{70}Kr and ^{74}Sr, where we obtain a value below experiment. Since in these cases, the daughter nuclei are odd-odd $N = Z$, one may argue that the observed jump from the regular trend in Q_{EC} is due to an extra neutron-proton binding, which is not taken into account in the present calculation. The discrepancy found in the half-lives of the most unstable nuclei is related to the discrepancy found in the Q_{EC} value.

We finally present and discuss the results obtained for the $B(GT^+)$ strength distributions in the iron mass region. In this case, the two coupling strengths of the ph and pp residual interactions have been determined to reproduce the positions of the experimental $B(GT^+)$ resonances as obtained from the (n,p) reactions. This has been done in a global way, choosing $\chi^{ph}_{GT} = 0.10$ MeV and $\kappa^{pp}_{GT} = 0.05$ MeV [4], as the best set of values within a deformed HF basis with the force SG2 that reproduce the observed resonances in the set of nuclei considered in this work. We note that the value of χ^{ph}_{GT}, which mainly determines the position of the resonance, is smaller than the typical values expected from systematic fits [17] or from consistency with the SG2 mean field [1]. This feature was already pointed out in Ref. [17], where the coupling strengths χ^{ph}_{GT} needed to reproduce the GT giant resonances were found to be smaller than the fitted A^{-1} law, in the mass region under consideration in this work.

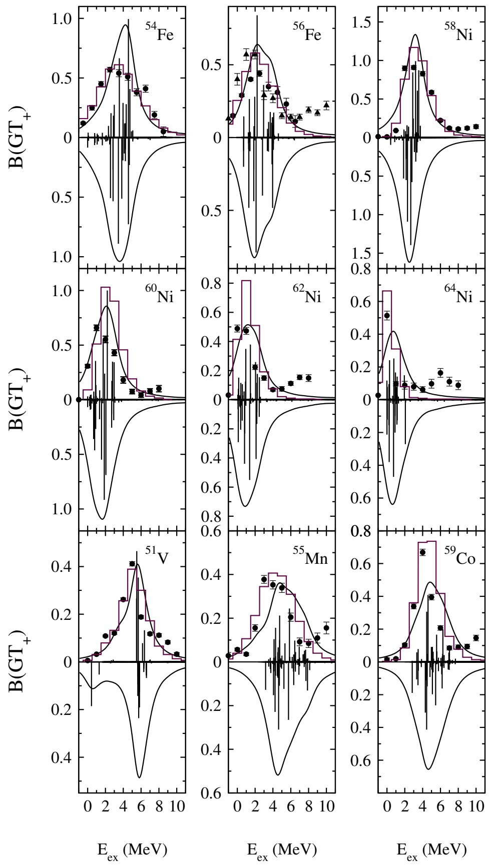

Figure 6. Gamow-Teller strength distributions plotted versus the excitation energy of the corresponding daughter nucleus. The results are plotted downward in the case of HF+BCS approximation and upward in the case of HF+BCS+QRPA. Results from full shell model diagonalization are shown by histograms.

The results obtained for the $B(GT^+)$ strength distributions can be seen in Fig. 6. Plotted downward are the results of uncorrelated two-quasiparticle (HF+BCS) calculations, both individual and folded strengths. Plotted upward are the data [18], accumulated in 1 MeV bins (dots with error bars), as well as the $B(GT^+)$ strengths obtained from correlated two-quasiparticle (HF+BCS+ QRPA) calculations. Also shown for comparison as histograms are the results from full Shell Model diagonalization of Ref. [19]. Though the $B(GT^+)$ strength distributions obtained from full Shell Model calculations may agree better with experiment in some details, the present HF+BCS+QRPA results are, on the overall, of comparable quality. The agreement with experiment is in general quite satisfactory. We can see that the experimental $B(GT^+)$ strength distributions are fragmented over many states and that the centroids and widths of the distributions are well reproduced in our calculations [4].

5. Magnetic dipole M1 excitations

Inelastic proton scattering experiments were first performed [20] at low excitation energies to confirm the orbital nature of the low-lying states. These measurements were extended [21] to higher energies indicating the existence of considerable spin strength (about 11 μ_N^2) between excitation energies ranging from 5 to 10 MeV in several rare-earth nuclei. The distribution of the strength in this energy range exhibits a double-humped structure in most nuclei.

The results for the rare-earths are shown in Fig. 7 for ^{150}Nd, ^{154}Sm, ^{156,158}Gd and ^{168}Er.

The experimental data exhibit in most nuclei a double-humped structure that is well described theoretically [10]. The unperturbed ($H_{SS} = 0$) spin $M1$ strength distribution is displayed in each plot by a dotted curve, while that obtained with the consistent spin-spin residual interaction ($K_S = 88$ MeV, $q = -0.95$) is shown with a solid line.

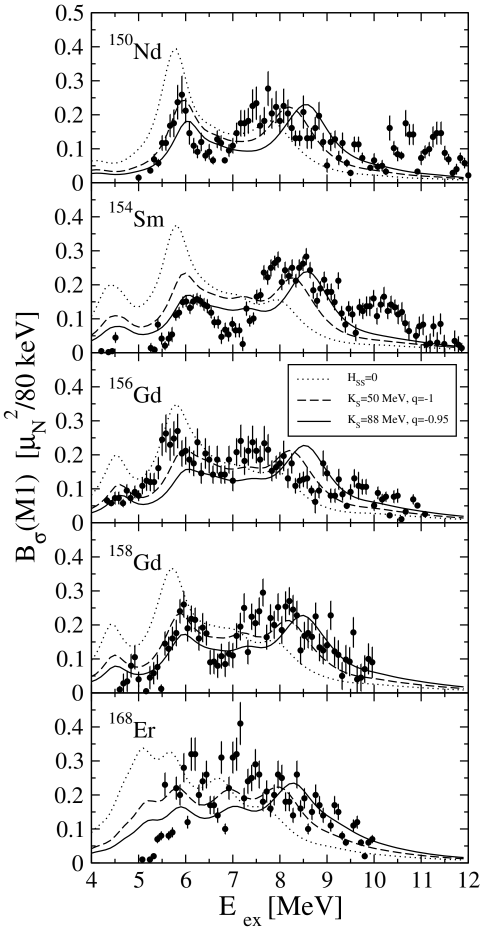

Figure 7. Energy distribution of the spin $M1$ strength with $K^\pi = 1^+$ obtained with the force SG2 in the rare earths ^{150}Nd, ^{154}Sm, ^{156,158}Gd and ^{168}Er for various choices of the spin-spin residual interaction. Experimental data are from Ref.[21].

6. Conclusions

We have applied a selfconsistent deformed HF+BCS+QRPA formalism with density-dependent two-body effective Skyrme interactions to the description of β-decay properties in various isotopic chains of medium-mass proton-rich nuclei, as well as to the study of Gamow-Teller strength distributions in the iron mass region. We have also studied within the same formalism spin magnetic dipole excitations. This approximation has the appealing feature of treating the excitations and the ground state in a selfconsistent framework with basically no free parameters. This feature is particularly interesting for nuclei far from stability, where extrapolations of methods based on local fits are doubtful.

Very reasonable agreement with ground state, $\beta-$decay properties, as well as with GT and spin $M1$ strength distributions is obtained. In the $A \sim 70$ mass region we have found shape isomerism in most of the isotopes studied and a very reasonable agreement with available experimental data on Q_{EC} values, half-lives, and GT strength distributions. From our study of the dependence on the shape of the GT strength distributions we conclude that information on the shape of the parent nucleus can be gained by comparison with experiment in the whole Q_{EC} window.

Concerning the iron mass region, we have found that we need a very small residual interaction to reproduce the data. This implies that the bare two quasiparticle approximation is already a fairly good approximation here. Although the full Shell Model calculations might be superior in this region, and some fine details of data may be better described, we find that on the overall the agreement with experiment of present QRPA calculations is comparable. Our approach has the advantage that can be extended to much heavier nuclei beyond the current capability of the full Shell Model, without increasing the complexity of the calculations.

We also studied the energy distributions of the spin $M1$ strength and the similarities and differences with their GT counterparts.

Acknowledgments

This work was supported by Ministerio de Ciencia y Tecnología (Spain) under contract number BFM2002-03562.

References

1. P. Sarriguren *et al.*, Nucl. Phys. A **635** (1998) 55; A **658** (1999) 13.
2. P. Sarriguren, E. Moya de Guerra and A. Escuderos, Nucl. Phys. A **691** (2001) 631.
3. P. Sarriguren, E. Moya de Guerra and A. Escuderos, Phys. Rev. C **64** (2001) 064306.
4. P. Sarriguren, E. Moya de Guerra and R. Alvarez-Rodriguez, Nucl. Phys. A **716** (2003) 230.
5. D. Vautherin and D. M. Brink, Phys. Rev. C **5** (1972) 626; D. Vautherin, Phys. Rev. C **7** (1973) 296.
6. P. Quentin and H. Flocard, Annu. Rev. Nucl. Part. Sci. **28** (1978) 253; P. Bonche *et al.*, Nucl. Phys. A **443** (1985) 39.
7. M. Beiner *et al.*, Nucl. Phys. A **238** (1975) 29.
8. N. Van Giai and H. Sagawa, Phys. Lett. B **106** (1981) 379.
9. M. Hirsch *et al.*, Nucl. Phys. A **535** (1991) 62; K. Muto *et al.*, Z. Phys. A **341** (1992) 407.
10. P. Sarriguren, E. Moya de Guerra and R. Nojarov, Phys. Rev. C **54** (1996) 690; Z. Phys. A **357** (1997) 143.
11. D. Cha, Phys. Rev. C **27** (1983) 2269; J. Engel, P. Vogel and M.R. Zirnbauer, Phys. Rev. C **37** (1988) 731; K. Muto and H.V. Klapdor, Phys. Lett. B **201** (1988) 420.
12. J. Krumlinde and P. Möller, Nucl. Phys. A **417** (1984) 419.
13. P. Moller and J. Randrup, Nucl. Phys. A **514** (1990) 1.
14. A. Bohr and B. Mottelson, *Nuclear Structure*, (Benjamin, New York, 1975).
15. H. Flocard *et al.*, Nucl. Phys. A **203** (1973) 433.
16. G. Audi and A.H. Wapstra, Nucl. Phys. A **595** (1995) 409; G. Audi *et al.*, Nucl. Phys. A **624** (1997) 1.
17. H. Homma *et al.*, Phys. Rev. C **54** (1996) 2972.
18. M.C. Vetterli *et al.*, Phys. Rev. C **45** (1992) 997; C **40** (1989) 559; T. Rönnqvist *et al.*, Nucl. Phys. A **563** (1993) 225; W.P. Alford *et al.*, Phys. Rev. C **48** (1993) 2818; S. El-Kateb *et al.*, Phys. Rev. C **49** (1994) 3128; A.L. Williams *et al.*, Phys. Rev. C **51** (1995) 1144.
19. E. Caurier *et al.*, Nucl. Phys. A **653** (1999) 439.
20. C. Djalali *et al.*, Phys. Lett. B **164** (1985) 269.
21. D. Frekers *et al.*, Phys. Lett. B **244**, 178 (1990); A. Richter, Prog. Part. Nucl. Phys. **34** (1995) 261.